

Application of Improved APO Algorithm in Vulnerability Assessment and Reconstruction of Microgrid

Jili Xie¹, Hailing Ma^{2,*}

¹Key Laboratory of Engineering Dielectrics and Its Application, Ministry of Education, Harbin University of Science and Technology, Harbin Heilongjiang, China

²Institute of Nuclear and New Energy Technology, Tsinghua University

Abstract. Artificial Physics Optimization (APO) has good global search ability and can avoid the premature convergence phenomenon in PSO algorithm, which has good stability of fast convergence and robustness. On the basis of APO of the vector model, a reactive power optimization algorithm based on improved APO algorithm is proposed for the static structure and dynamic operation characteristics of microgrid. The simulation test is carried out through the IEEE 30-bus system and the result shows that the algorithm has better efficiency and accuracy compared with other optimization algorithms.

Keywords: Microgrid, vulnerability assessment system, reconfiguration, artificial physics optimization.

1. Introduction

The reconfiguration of microgrid is the precondition of meeting the basic requirements of line voltage, current and the operation of power grid in the radiation state, optimizes microgrid operation by changing the load in the network (adjustable load and interruptible load), the line switch and the state of Point of Common Coupling (PCC) to satisfy the sensitive load power quality, improve the node voltage offset, eliminate line overload etc. So the microgrid vulnerability assessment is to find out the weak link of the microgrid, to enhance its security and stability, and guide the reconfiguration work of microgrid, so as to improve the reliability of the network in normal operation, and restore the user's power supply as soon as possible when the fault occurs.

The mosaic physics algorithm has good global search ability, and the optimization process avoids the premature convergence of the particle swarm algorithm, which has good stability, fast convergence and robustness. Taking the IEEE 30-bus system as an example, the simulation results are compared and the results are compared. The results show that the algorithm has the advantages of fast convergence speed and high precision.



2. Vulnerability Analysis of Microgrid

2.1. Microgrid Modeling and Power Flow Analysis

There are two kinds of operation modes of microgrid, and the microgrid model and power flow calculation in different operating modes is different. In the network operation mode, the large power grid as the "balance node" of the microgrid. And when the microgrid is in the island mode, the microgrid will not exist in the balance node, it is necessary to carry out detailed modeling of the island microgrid.

Different from the traditional generator, microgrid distributed power generation device and power electronic converter and output filter device connected through a certain control strategy to access the grid operation. It can be equivalent to an ideal voltage source, through the output impedance connected to the microgrid, as shown in Figure 1.

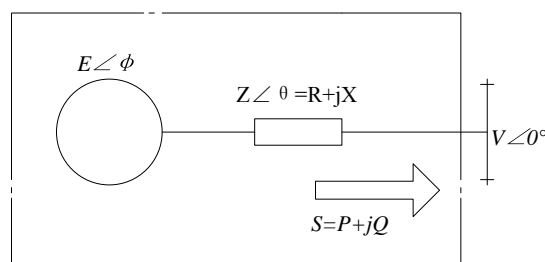


Fig.1 Equivalent circuit of a micro-source

The active power and reactive power of DG output can be expressed as:

$$P = \frac{EV}{R} - \frac{V^2}{R} \quad (1)$$

$$Q = -\frac{EV}{Z} \phi \quad (2)$$

Because DG is connected to the power grid via control of the control strategy, the output power can be controlled according to the following formula.

$$Q_{Gi} = \frac{1}{m_p} (V_i^* - |V_i|) \quad (3)$$

$$Q_{Gi} = \frac{1}{n_q} (\omega^* - \omega) \quad (4)$$

In the formula (3), V^* is the rated voltage amplitude; m_p is the active power static control coefficient; P_{Gi} is the three-phase injected active power of D_{Gi} ; ω is the angular frequency of DG output voltage; ω^* is the rated angular frequency.

In the calculation of the current flow, the branch current, the three-phase injection power of the bus and the bus injection current of the microgrid are calculated by the formula (5) and the formula (7) respectively.

$$I_{ij}^{abc} = Y_{ij}^{abc} V_{ij}^{abc} \quad (5)$$

$$S_i^{abc} = V_i^{abc} (I_i^{abc})^* \quad (6)$$

$$I_{i,inj}^{abc} = \sum_{\substack{j=1 \\ j \neq i}}^{nb} I_{ij}^{abc} \quad (7)$$

Substituting formulas (5) and (7) into formula (6) yields the a-phase transmission power, the power calculation of the b-phase and the c-phase is given by reference to formulas (8) and (9). Combined with the formulas (3) to (11), the three-phase power flow calculation of microgrid is carried out, which lays the foundation for the subsequent vulnerability analysis and reconstruction calculation.

$$P_i^a = \sum_{\substack{j=1 \\ j \neq i}}^{nb} \sum_{ph=a,b,c} [V_i^a |Y_{ij}^{a(ph)-n}| V_i^{(ph)} \cos(\theta_{ij}^{a(ph)} + \phi_i^{(ph)} - \phi_i^a) - |V_i^a |Y_{ij}^{a(ph)-n}| V_j^{(ph)} \cos(\theta_{ij}^{a(ph)} + \phi_j^{(ph)} - \phi_i^a)] \quad (8)$$

$$Q_i^a = \sum_{\substack{j=1 \\ j \neq i}}^{nb} \sum_{ph=a,b,c} [V_i^a |Y_{ij}^{a(ph)-n}| V_i^{(ph)} \sin(\theta_{ij}^{a(ph)} + \phi_i^{(ph)} - \phi_i^a) - |V_i^a |Y_{ij}^{a(ph)-n}| V_j^{(ph)} \sin(\theta_{ij}^{a(ph)} + \phi_i^{(ph)} - \phi_i^a)] \quad (9)$$

$$0 = P_{Li}^{abc} - P_{Gi}^{abc} + P_i^{abc}(\omega, V_i^{abc}, V_j^{abc}, \phi_i^{abc}, \phi_j^{abc}) \quad (10)$$

$$0 = Q_{Li}^{abc} - Q_{Gi}^{abc} + P_i^{abc}(\omega, V_i^{abc}, V_j^{abc}, \phi_i^{abc}, \phi_j^{abc}) \quad (11)$$

In the formula (8) to (11), P_i and Q_i are divided into a-phase transmission active power and reactive power of bus i ; P_{Li} , Q_{Li} are active power and reactive power of load i .

2.2. Microgrid Structural Parameter Vulnerability Index

The principle of grid topology can be simply described as: node represents generator, load and substation, and side represents transmission line. Introducing the line weight and defining the shortest path is the path that minimizes the sum of the line weights between the generator node and the other nodes,

$$\text{Min} \sum_{i \in L} R_i \quad (12)$$

The node number and the line profile are defined as the sum of the shortest path times through the node or line. Network in a unit from its topology to exit the time is t_{os} , and then there is a network topology failure time probability can be expressed as:

$$\gamma_{os} = \frac{t_{os}}{T_s} \quad (13)$$

Here γ_{os} as a microgrid vulnerability index is one of the index, because γ_{os} value and vulnerability is proportional to the relationship between the efficiency from the working hours, the longer the cumulative time to exit the network, the more fragile the component. γ_{os} is more direct, that γ_{os} value is greater, the more vulnerable the unit.

2.3. Microgrid operating state vulnerability index

Microgrid operating state vulnerability refers to the ability of a microgrid to maintain its topology stability after a certain unit or some unit of the microgrid is withdrawn or withdrawn in a certain operating mode.

2.3.1. Node voltage quality index

To provide users with a variety of power quality is an important feature of microgrid, and different types of nodes on the power quality requirements are also different, especially sensitive to the most demanding. The node voltage quality index is characterized by the distance between the current voltage value of each node and the maximum allowable voltage offset value of the node. The larger the index value indicates that the node is more unstable, and its expression is:

$$DI_i = \sum_{i=1}^{NB} \frac{|V_i| - |V_i^{sp}|}{\Delta V_i^{\lim}} \quad (14)$$

In the formula (14), NB is the number of nodes; V_i is the node running voltage; V_i^{sp} is the rated voltage of the node; ΔV_i^{\lim} is the maximum allowable voltage offset required to guarantee the node power quality, and the voltage offset value of each node is different.

2.3.2. Line energy transmission index

The design concept of microgrid is around the whole system energy demand, so in the microgrid disturbance or failure, in order to ensure that the micro-grid can carry out energy transmission, the energy transfer index of the line is represented by the ratio of "line transmission power" and "maximum transmission power". The expression is:

$$OL_i = \sum_{i=1}^{NL} \frac{P_{li}}{P_{li}^{\lim}} \quad (15)$$

In the formula, NL is the number of lines; p_{li} is the branch transmission power; p_{li}^{\lim} is the maximum power that the branch can transmit.

As the microgrid exists in the network mode and island mode, so in the network mode, PCC switch branch flow power and microgrid energy storage device supply power ratio greater, micro-power grid itself, the greater the power shortage; , The microgrid current power shortage and energy storage device, the greater the ratio of the power supply, the more vulnerable the grid, so the definition of PCC branch line energy transmission indicators:

$$OL_i = \begin{cases} \frac{P_{PCC}}{E_{c0}} & \text{Networking mode} \\ \frac{\Delta P_I}{E_{I0}} & \text{Island mode} \end{cases} \quad (16)$$

In the formula, P_{PCC} is the power flowing through the PCC branch switch in the network operation mode; ΔP_I is the power shortage of the microgrid in the islanding mode; E_{c0} and E_{I0} are the recharge power in the energy storage device in the network and island mode respectively.

2.4. Comprehensive Evaluation System of Microgrid Vulnerability

The establishment of microgrid vulnerability evaluation system is shown in Fig 2. The comprehensive vulnerability of microgrid is defined as the product of the operational state vulnerability index V_o and the structural vulnerability index V_s , where V_o is defined as the weighted sum of each index, V_s is defined as the product of each index, the weight coefficient is solved by the level judgment matrix.

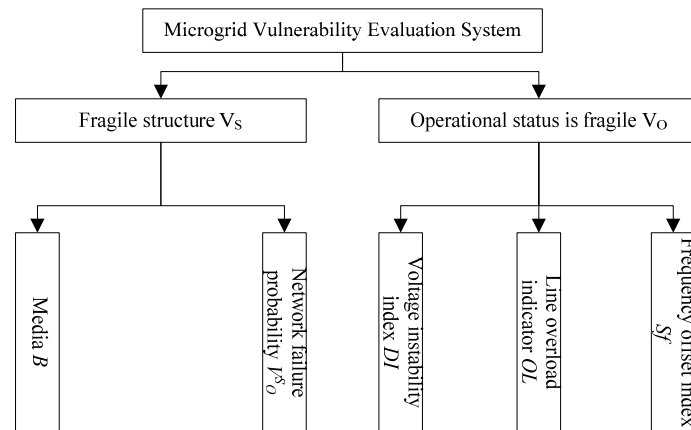


Fig.2 Vulnerability assessment system of microgrid

The fragility of unit i and the comprehensive vulnerability of microgrid are calculated as:

$$ISV = V_s V_o = B_i \gamma_{os} (\omega_1 DI_i + \omega_2 Sf_i + \omega_3 OL_i) \tag{17}$$

$$ISV = \sum_{i=1}^{NB, NL} ISV_i \tag{18}$$

In the formula, ISV_i is the fragility of unit i ; $\omega_1, \omega_2, \omega_3$ are the weight coefficients of each running state vulnerability index respectively; ISV is the comprehensive fragility of microgrid.

3. Real - time Reconstruction Model of Microgrid Based on Vulnerability Evaluation

3.1. Mathematical model

Microgrid normal operation, its fragile value is random fluctuations in the change. Scheduling personnel through real-time control and reconstruction to change the PCC switch, branch switch and contact switch, so at any time in 1 day to give the optimal grid, and the network mode and island mode switch, so as to adapt to microgrid Operation State of change. Therefore, the real-time reconstruction mathematical model of microgrid based on vulnerability assessment can be expressed as:

$$\min I_{SV} = f(t, X_{PCC}, X_i) = \int \sum (\omega_1 B_{n,i} V_{11,i} + \omega_2 B_{l,i} V_{12,i}) dt \tag{19}$$

$$I_{SV}(t) = \lim_{t_1 \rightarrow t_2} \sum_{i=1}^N (\omega_1 B_{n,i} V_{11,i}(t) + \omega_2 B_{l,i} V_{12,i}(t)) \quad \text{s.t.} \quad P_{G,i \min} \leq P_{G,i} \leq P_{G,i \max}, i = 1, \dots, n \tag{20}$$

In the formula: X_i for the microgrid branch switch state (open to 0, closed to 1); X_{PCC} for the realization of microgrid networking/island operating mode smooth switching switch point state (open 0, closed to 1); $P_{G,i}$ and $Q_{G,i}$ are the active and reactive power of the generator respectively; D is the load demand vector; g_k is the current network structure; G_k is the set of all allowed connected radial network configurations.

3.2. Cell bat algorithm

The mini-bats use the time delay and the time difference between the ears and the loudness of the echo to emit the echo to establish the three-dimensional scene of the surrounding environment. The bats algorithm changes the behavior of the bats by frequency tuning and the size of the pulse transmission frequency. When the condition is satisfied, it automatically switches from global search to local search, thus realizing the mutual conversion between global search and local search in dynamic control. Once a solution (bat) is selected from the existing optimal solution, the new position of the bat is:

$$x_{new}(i) = x_{old} + \xi A^t \quad (21)$$

In the formula: x_{old} is a solution randomly selected from the current optimal solution set; A^t represents the average of the current bat population's loudness; x_{new} is the new solution for the update.

The loudness $A(i)$ and the firing rate $R(i)$ of the pulses are updated as the iterative process proceeds. Usually, in the process of approaching the prey, the loudness will gradually decrease, the rate of pulse transmission will gradually increase, $A(i)=0$ means that the bat i just found a prey, temporarily stop sending any sound. The update formula for the pulse loudness and emission rate is:

$$A^{t+1}(i) = \alpha A^t(i) \quad (22)$$

$$R^{t+1}(i) = R^0(i) \times (1 - e^{-\gamma}) \quad (23)$$

In the formula: $0 < \alpha < 1$, $\gamma > 0$, are constant; $A^{t+1}(i)$ and $A^t(i)$ are $t+1$ time and t moment of the pulse loudness.

The cells and their neighbors are introduced into the local search of the algorithm to form CBA (cellular bat algorithm). The bats scattered in the cell space are also optimized in the context of their neighbors, and the CBA combines the cell, the cell space with the search space of the cell neighbors and the bat, and the set of feasible solutions. For cell space, where any element is treated as a cell and the cell neighbor uses the extended Moore neighbor type.

4. Improved APO

APO is the United States Wyoming State University Spear WM and others by Newton's second law inspired by an optimization algorithm. Each of the individuals in the algorithm is a feasible solution in the solution space. Each individual according to their own inertia and other individuals together to adjust their own movement, the whole group experienced the best position is to find the global optimal solution, and the individual's good and bad by the optimization of the problem to assess the value. The Each good individual attracts individuals smaller than it, while poor individuals' exclusion is better than its individual. Each individual updates its own quality according to the global fitness value and its own fitness value, thus updating the individual's speed and position. The APO algorithm with search vector increases the population diversity of the algorithm by introducing the velocity vector of the individual, which effectively improves the global search ability of the algorithm and has fast convergence and robustness.

In the vector model of the APO algorithm, assuming that the population size is n , the mass of the individual i ($i = 1, 2, n$) is expressed as m_i , m_i can be obtained by the following formula.

$$m_i = e^{\frac{f(x_{best}) - f(x_i)}{f(x_{worst}) - f(x_{best})}} \quad (24)$$

Let the direction of the individual j relative to the individual i in the k th dimension be expressed as:

$$r_{ij,k} = \begin{cases} 1, X_{i,k} > X_{j,k} \\ 0, X_{i,k} = X_{j,k} \\ -1, X_{i,k} < X_{j,k} \end{cases} \quad (25)$$

The direction vector of the individual j relative to the individual i is:

$$r_{ij} = [r_{ij,1} r_{ij,2} \cdots r_{ij,n}]^T \quad (26)$$

Thus, we can get the vector of the force of the individual j on the individual i as:

$$F_{ij} = \begin{cases} Gm_i m_j \|x_j - x_i\| r_{ij}, \text{ if } j \in N_i \\ -Gm_i m_j \|x_j - x_i\| r_{ij}, \text{ if } j \in M_i \end{cases} \quad (27)$$

In the formula, G is the gravitational constant, usually the value of G=10.

Then the individual i in the k-dimensional speed and position vector expression is:

$$V_i(t+1) = wV_i(t) + \alpha \sum_{j=1, j \neq i}^{N_{pop}} F_{ij} / m_i \quad (28)$$

$$X_i(t+1) = X_i(t) + V_i(t+1) \quad (29)$$

Formula: w is the inertia weight, α is a random variable, and α obeys N(0, 1) Standard normal distribution.

The change of the inertia weight w will affect the search ability of the algorithm, and the w is large, then the global search ability is better; w is smaller, then the local search ability is better. In order to balance the global search ability and local search ability of the individual, the inertia weight w in the algorithm decreases dynamically with the iteration. The expression is:

$$w = 0.9 - \frac{iter-1}{Maxiter} 0.5 \quad (30)$$

Where: iter is the current iteration number; Maxiter is the maximum number of iterations.

5. Analysis of Examples

In order to verify the validity and feasibility of the proposed algorithm, this paper uses IEEE30 node system to carry out numerical simulation analysis. The system consists of six generator nodes (1,2,5,8,11,13), four adjustable transformer branches (6-9, 6-10, 4-12, 27-28) and nine (10,12,15,17,20,21,23,24,29), the system branch detailed parameters see the literature [4]. In this paper, the following modifications are made to the node system: the branch 2-6 is modified to the DC line shown in the figure 4, where the rectifier station is connected at node 2, the inverter station is connected at node 6 of the inverter station as a DC system reference voltage node. A compensating device has been installed in the converter station to provide the reactive power consumed by its commutation. DC control system operation mode: rectifier side constant current control (1p.u.), inverter side set out of arc control (15°). The conversion ratio of the converter transformer is 15%, and the adjustment amount is 1.25%. The algorithm is used to optimize the reactive power of the algorithm and compared with the optimized results of PSO and GA. The population size of this algorithm is 30, the maximum number of iterations

is 200, the particle size of the particle swarm algorithm is 30, the maximum number of iterations is 200, the population size of the genetic algorithm is 50, the maximum number of iterations is 200, 0.8, the probability of mutation is 0.15.

It can be seen from Table 1 that the network loss of the system is reduced by 5.58% after optimization with particle swarm optimization algorithm, and the network loss of the system is reduced by 5.19% after optimization by genetic algorithm. The algorithm reduces the network loss by 6.74%. It is shown that under the same conditions, the optimization results obtained by particle swarm optimization and genetic algorithm are similar. The optimal solution obtained by the proposed algorithm is more ideal than the optimization results of the previous two algorithms.

Table 1. Comparison of AC/DC system parameters before and after optimization

being optimized	before being optimized	after being optimized		
		PSO	GA	Our algorithm
Active loss /p.u.	0.0635	0.0598	0.0602	0.0592
Optimize time /s		12.58	13.23	11.78

It can be seen from Fig. 3 that the genetic algorithm is ladder-like due to the intersection and variation of the individual, and the convergence rate is relatively slow and the optimal result has a large randomness. The convergence speed of the particle swarm algorithm is faster, and the optimal value is reached, which makes it easy to fall into the local optimum. The convergence rate of this algorithm is the fastest and not easy to fall into the local optimum. It can be seen that the improved mimicry physics algorithm proposed in this paper has some advantages to solve the reactive power optimization problem of power system and can meet the requirements of reactive power optimization.

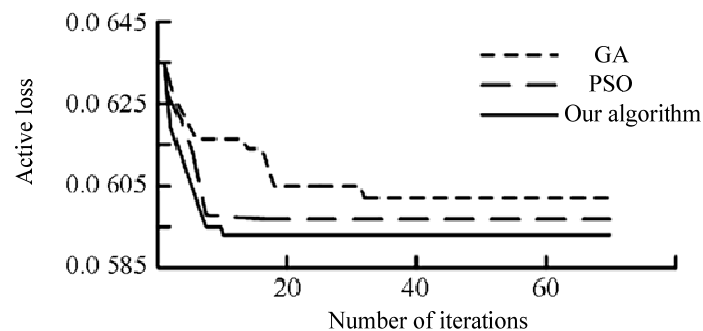


Fig.3 Performance characteristics curve of three optimization algorithms

6. Conclusion

Based on the static structure characteristics and dynamic operation characteristics of the microgrid, this paper establishes the comprehensive vulnerability evaluation system of the microgrid, and builds a reconstructed mathematical model considering the microgrid vulnerability. Based on the mimicry physics algorithm of the vector model, a reactive power optimization algorithm based on improved mimicry physics algorithm is proposed. By introducing the infeasible function and the multidimensional search method with the contraction factor, the difficulties caused by the penalty function method are discussed. And the algorithm avoids the frequent convergence of the particles and other algorithms, which has good stability and robustness.

References

- [1] Chinchilla M, Arnaltes S, Burgos J C. Control of permanent-magnet generators applied to variable speed wind-energy systems connected to the grid [J]. IEEE Transactions on Energy Conversion, 2014, 21 (1): 130- 135.
- [2] Wang Chengshan, Li Xialin, Guo Li, et al. A seamless operation mode transition control strategy for a microgrid based on master-slave control [J]. Science china (Techno. Sciences), 2012, 55 (6): 1644-1654.
- [3] MOMOH J, GUO S X, OGBUOBIRI E C, et al. The quadratic interior point method solving power system optimization problems [J]. IEEE Transactions on Power Systems, 2004, 9 (3): 1327-1336.
- [4] GRANVILLE S. Optimal reactive dispatch through interior point methods [J]. IEEE Transactions on Power Systems, 2004, 9 (1): 136-146.
- [5] DEEB N, SHAHIDEPOUR S M. Linear reactive power optimization in a large power network using the decomposition approach [J]. IEEE Transactions on Power Systems, 2010, 5 (2): 428-438.
- [6] XIE LP, ZENG JC, CUI Z H. The vector model for artificial physics update algorithm for global optimization problems [C] // The 10th International Conference on Intelligent Data Engineering and Automated Learning, Spain, Sept. 2009: 610- 617.